Journal of Microencapsulation

http://informahealthcare.com/mnc
ISSN: 0265-2048 (print), 1464-5246 (electronic)

J Microencapsul, 2013; 30(8): 728–740
© 2013 Informa UK Ltd.
DOI: 10.3109/02652048.2013.788081

informa healthcare

Microencapsulation of alpha-mangostin into PLGA microspheres and optimization using response surface methodology intended for pulmonary delivery

Aimen Abdo Elsaid Ali, Muhammad Taher, and Farahidah Mohamed

Department of Pharmaceutical Technology, Kulliyyah of Pharmacy, International Islamic University Malaysia, Kuantan, Pahang, Malaysia

Abstract

Documented to exhibit cytotoxicity and poor oral bioavailability, alpha-mangostin was encapsulated into PLGA microspheres with optimization of formulation using response surface methodology. Mixed levels of four factors Face central composite design was employed to evaluate critical formulation variables. With 30 runs, optimized formula was 1% w/v polyvinyl alcohol, 1:10 ratio of oil to aqueous and sonicated at 2 and 5 min time for primary and secondary emulsion, respectively. Optimized responses for encapsulation efficiency, particle size and polydispersity index were found to be 39.12 ± 0.01%, 2.06 ± 0.017 μm and 0.95 ± 0.009, respectively, which matched values predicted by mathematical models. About 44.4% of the encapsulated alpha-mangostin was released over 4 weeks. Thermal analysis of the microspheres showed physical conversion of alpha-mangostin from crystallinity to amorphous with encapsulated one had lower *in vitro* cytotoxicity than free alpha-mangostin. Aerodynamic diameter (784.3 ± 7.5 nm) of this alpha-mangostin microsphere suggests suitability for peripheral pulmonary delivery.

Keywords

Factorial design, inhalation, lung cancer, xanthones

History

Received 8 May 2012
Revised 6 March 2013
Accepted 11 March 2013
Published online 30 April 2013

Journal of Microencapsulation Downloaded from informahealthcare.com by University of Laval on 05/25/14
For personal use only.

Introduction

Despite numerous studies on anti-cancer agents, lung tumour remains one of the most common killers throughout the world (Zu et al., 2009; Jemal et al., 2011). Clinically used anti-cancers administered parenterally as free drug solutions inherit many problems including normal tissue toxicity, lack of specificity and susceptibility to induce drug resistance (Wong et al., 2007). Targeting the drugs by enhancing its specificity seems to be a promising approach to minimize the undesirable effects with improved drug bioavailability. This can be achieved by micro-encapsulation of the therapeutic agents into biodegradable polymers customized to appropriate size range with or without ligand attached to it. For instance, highly potent cytotoxic drug, doxorubicin, demonstrated non-selective distribution in cancerous and healthy tissue leading to severe side effects when administered as a free drug. However, its corresponding conjugated form, formulated as PLGA nanoparticles, demonstrated significant reduction in undesirable effects against HepG2 cells (Yoo et al., 2000).

In this study, we attempted to encapsulate a potent natural product-based cytotoxic agent, alpha-mangostin, which is abundantly found in the inedible parts of Garcinia species. It can also be naturally obtained from the stem bark of *Garcinia malaccensis* (Taher et al., 2012) or chemically synthesized (Iikubo et al., 2002). Its anti-proliferative activities were demonstrated against numerous cell lines including human colonic cancer, DLD-1 cells (Akao et al., 2008), breast cancer, BC-1 cells, small-cell lung cancer, NCI-H187 (Suksamrarn et al., 2006) and human lung adenocarcinoma A549 cells (Shih et al., 2010). In addition, it was found to possess many therapeutic properties namely analgesic (Cui et al., 2010), anti-inflammatory (Chen et al., 2008), anti-fungal (Kaomongkolgit et al., 2009) and anti-bacterial activities (Sakagami et al., 2005). Furthermore, alpha-mangostin was reported to exert anti-oxidative (Williams et al., 1995; Mahabusarakam et al., 2000; Jung et al., 2006; Pedraza-Chaverri et al., 2009) and neuroprotective effects (Pedraza-Chaverri et al., 2009; Wang et al., 2012). Interestingly, alpha mangostin had also been used in combination with doxorubicin to mitigate toxicity of doxorubicin against healthy cells (Tangpong et al., 2011).

Nevertheless, it had been reported that alpha-mangostin was rapidly distributed to the rat tissue following intravenous administration explaining its low oral bioavailability and short circulating half-life attributed to its lipophilic nature. To date, only recently, attempt was made applying solid dispersion concept to enhance water solubility of alpha-mangostin through coupling it with water-soluble polymer, polyvinylpyrrolidone (PVP), to form nanomicelle. However, the previous studies had not addressed the issue of short half-life and low oral bioavailability. Therefore, the aim of this study was to encapsulate alpha-mangostin into PLGA microsphere as a preliminary approach to extend its half-life and probably its bioavailability. Multiple emulsion solvent evaporation was employed to synthesize the microspheres to the size distribution desirable for pulmonary delivery that was envisaged to provide controlled release of the therapeutic agent passively targeting the bronchopulmonary region. On contact with the mucous membrane of the pulmonary

Address for correspondence: Farahidah Mohamed, International Islamic university Malaysia, Pharmaceutical Technology Department, Kulliyyah of Pharmacy, International Islamic University Malaysia, Bandar Indera Mahkota, 25200 Kuantan, Pahang, Malaysia. E-mail: farahidah@iium.edu.my

Copyright Informa Healthcare 2013
Not for Sale or Commercial Distribution

region, the microsphere was expected to release alpha-mangostin in a gradual manner from the slowly dissolving microspheres and hence extending its half-life and bioavailability. Nevertheless, the scope of this study focuses on fabrication, optimization and characterization of the particles only. The potential route of administration via pulmonary was also assessed simply based on its aerodynamic diameter. In addition, the degree to which this microsphere may influence its half-life and bioavailability will be subjects of our future studies.

With respect to delivering the micro-carrier particles into the pulmonary region, the desired aerodynamic diameter of range 1–5 μm is crucial to ensure deposition at the lung periphery since the submicron particles have the ability to be suspended in air and exhaled, while larger particles are held in oropharynx (Mohamed and Van Der Walle, 2008; Emami et al., 2009). The study utilized response surface methodology (RSM) employing the central composite design (CCD) of mixed-levels of four factors to elucidate critical processing parameters reflected in responses obtained.

Although single emulsion method was the most commonly employed technique for encapsulation of lipophilic substances, high drug loading of the latter may result in re-crystallization of the compound during the solvent evaporation process, which in turn leads to perforation of the particle wall by drug needle (Wischke and Schwendeman, 2008). Therefore, double emulsion solvent evaporation method was employed here instead of single emulsion in order to reduce the porosity of loaded particles that also mitigated the burst effect as well as prolong the drug release.

Materials and methods

Materials

The co-polymer PLGA (50:50, 0.4 dl/g) was purchased from PURAC® (Holland, The Netherlands). Polyvinyl alcohol (PVA) with a molecular weight of 115 kDa (degree of hydrolysis 87%) was purchased from BDH Chemicals (England, UK). Acetonitrile of high-performance liquid chromatographic (HPLC) grade was obtained from Fischer scientific (Leicestershire, UK). All other chemicals were of analytical grade. Alpha-mangostin was isolated from the stem bark of *G. malaccensis* as reported by Taher et al., 2012. The purity of the isolated alpha-mangostin was approximately 94% as identified by HPLC and compared to the reference standard of purity 96.5%. The latter was purchased from ChromaDex (Irvin, CA).

Experimental design

We employed mixed-levels of four factors using CCD of RSM to generate mathematical models following 30 runs. The factors that were the independent variables constituted of PVA concentration (X1), volume ratio of oil to aqueous phase in primary emulsion (X2) and sonication times for both primary (X3) and secondary emulsions (X4). Only the latter was tested against two levels, while the others tested against three levels. All factors were evaluated for the following responses: encapsulation efficiency (EE), particle size (PS) distribution, polydispersity index (SPAN). The models (Equation 1) were generated by Design-Expert software® version 8.0.7.1 (State-Ease Inc., Minneapolis, MN). Table 1 shows the independent variables with their respective levels. According to Murphy (2007), the mathematical relationship between the independent variables and the responses were described by the following quadratic polynomial equation:

$$Y = \beta_0 + \sum_{i=1}^{k} \beta_i X_i + \sum_{i=1}^{k} \beta_i X_i^2 + \sum_{i=1}^{k-1} \sum_{j>i}^{k} \beta_{ij} X_i X_j \qquad (1)$$

Table 1. Independent variables and their designated levels in RSM design.

Independent variables (factors)	Unit	Factors' symbols	Coded levels*		
			−1	0	1
PVA concentration†	% (w/v)	X_1	1	3	5
Volume ratio of oil to aqueous phase†	n/a	X_2	1:1	5:1	10:1
Sonication time†	Minute	X_3	1	2	3
Sonication time‡	Minute	X_4	3	–	5

*Levels −1, 0 and 1 represent low, intermediate (centre point) and high, respectively.
†Primary emulsion.
‡Secondary emulsion.

where Y is the response, β_0 represents the coefficient of the intercept and β_i refers to the estimated coefficient for the independent variables (X_i, $i = 1, 2, \ldots, k$), (X_j, $j > i$).

Model validation

The mathematical model was validated using check point analysis to assess its reliability in describing the characteristics of microspheres (Nasr et al., 2011). Briefly, five points were randomly chosen using the Design-Expert software (State-Ease Inc., Minneapolis, MN) since their predictive response values were derived within the low and high limit of 95% confidence interval. All formulations were characterized for their EE ($Y1$), particles size ($Y2$) and SPAN ($Y3$) as previously described followed by the calculation of bias based on the following equation, counted for each responses to envisage validity between actual and predicted values:

$$\text{Bias}(\%) = \frac{\text{Difference between actual and predicted values}}{\text{Actual value}} \times 100 \qquad (2)$$

Preparation of alpha-mangostin-loaded microspheres

A modified multiple emulsion–solvent evaporation technique was adopted as described by Harun et al. (2012). Briefly, 1% w/v alpha-mangostin was mixed by vortexing into 5% w/v PLGA previously dissolved in dichloromethane (DCM). To this oil phase, either 1, 3 or 5% w/v PVA was injected based on oil to aqueous volume ratios of 1:1, 1:5 and 1:10 and sonicated over ice bath at 40% amplitude (Cole-Parmer® 750-Watt Ultrasonic Processors; Chicago, IL) for either 1, 2 or 3 min. This primary emulsion was immediately injected into 10 times larger its volume, a secondary aqueous phase consisted of 1% w/v PVA and sonicated at either 3 or 5 min over ice bath. Finally, the double emulsion was transferred into a continuously stirred hardening tank operating at 500 rpm, and stirring was continued for 2 h to allow compete evaporation of DCM. The hardened microsphere was harvested by serial centrifugation at 1000, 3000 and 5000 rpm consecutively for 3 min each to remove larger particles, washed three times with purified water and lyophilized. The lyophilized microspheres were kept in air-tight amber glass container at 4 °C until further evaluation.

Determination of alpha-mangostin content in the microspheres

Alpha-mangostin was extracted from PLGA microspheres by first solubilizing these microspheres in acetonitrile and then precipitating the polymer by diluting with phosphate buffered saline (PBS) 30% (v/v). The supernatant containing the extracted alpha-

Journal of Microencapsulation Downloaded from informahealthcare.com by University of Laval on 05/25/14
For personal use only.

mangostin was filtered through 0.2 μm PTFE microfilter prior to analysis on the modified reverse phase HPLC (RP-HPLC) method as described by Ali et al. (2012). The EE was calculated based on the following equation:

$$\text{Encapsulation effeciency}\% = \frac{\text{Experimental concentration}}{\text{Theoretical concentration}} \times 100 \quad (3)$$

PS and SPAN

Prior to freeze-drying, the particles were subjected to size analysis by laser particle size analyzer BT-9300H (Bettersize Instruments Ltd., Liaoning, China). Size distribution was expressed as volume median diameter (d [v, 50]). The SPAN was calculated employing this equation: (d[v, 90] – d[v, 10])/d[v, 50], where d[v, 10], d[v, 50] and d[v, 90] represent the cumulative distribution of the PS at 10, 50 and 90% of total volume, respectively. Each sample was measured in triplicate.

Scanning electron microscope

The morphology of the optimized formulation of freeze-dried microspheres was assessed by scanning electron microscope (Carl Zeiss Evo® 50, Oberkochen, Germany) at an accelerating voltage of 5–10 KV and under high vacuum pressure. The samples were mounted on aluminium stub pre-pasted with double-sided carbon tapes and sputter-coated with a thin layer of gold prior to viewing to increase image contrast.

Characterization of aerodynamic diameter

Optimized formulation was subjected to the measurement of aerodynamic diameter by calculation based on the following equation: aerodynamic diameter $(d_a) = d\ \sqrt{\rho}$; where d = PS measured by laser diffraction and ρ = tapped density of the freeze-dried microspheres, measured by jolting volumeter (Copley JV 1000, Copley Scientific, Nottingham, UK), tapped for 5000×.

In vitro cytotoxicity study

A549 cell, a human non-small-cell lung adenocarcinoma cell line, was purchased from American Type Culture Collection (ATCC, Manassas, VA). The cells were grown in a complete medium containing Dulbecco's Modified Eagle Medium supplemented with 10% foetal bovine serum and 1% penicillin–streptomycin (10 000 units/ml–10 000 μg/ml, respectively) at 37°C under a humidified 5% CO_2 incubator.

The cytotoxicity of free alpha-mangostin and the loaded microspheres with alpha-mangostin were evaluated by measuring the cell viability using a modified 3-(4,5-dimethylthiazol-2-yl)-2,5-diphenyl-tetrazolium bromide (MTT) assay according to previously described method by Mosmann (1983). Briefly, A549 cells were seeded in 96-well micro-plates at a density of 1×10^4 cells/well and incubated for 24 h. Then, cells were treated with a serial dilution of free alpha-mangostin, namely 100, 50, 25, 12.5, 6.25, 3.13 and 1.56 μg/ml, in dimethyl sulfoxide (DMSO). For determination of cytotoxicity of alpha-mangostin microspheres, the cells were treated with the microspheres of equivalent concentration of 120, 60, 48, 36, 24, 12, 6, 3 and 1 μg/ml of the alpha-mangostin. The microspheres were presuspended in sterile PBS prior to loading into the cell. Incubation time following the loading was 48 h. The empty microspheres were used as the control. After the exposure period, the medium was withdrawn and the cells were washed with PBS and incubated with 20 μl of 5 mg/ml MTT solution for 4 h. The resultant water-insoluble formazan crystals were solubilised with 100 μl/well of DMSO. Then, the absorbance was measured by UV spectrophotometer at 560 nm and 650 nm (reference) using microplate reader. The percentage of cell viability was calculated based on the following equation. The cytotoxicity activities were expressed as the mean of three replicates ± standard error of the concentration of alpha-mangostin required to reduce cell viability by 50% (IC_{50}), which was calculated from the plot of the concentration versus corresponding cell viability. Data were analysed by four-parametric logistic equation using Sigma Plot software (version 11) (Systat Software Inc., San Jose, CA).

$$\text{Cell viability } (\%) = \frac{(\text{Absorbance of the sample} - \text{blank})}{(\text{Absorbance of the control} - \text{blank})} \times 100$$

In vitro release study

The *in vitro* release profile of the alpha-mangostin from the optimized formulation of PLGA-microspheres was conducted according to a previously described method (Bouissou et al., 2004). Five milligrams of microspheres with equivalent amount of approximately 0.5 mg alpha-mangostin were resuspended in 1 ml PBS (pH 7.4) containing 0.1% v/v Tween 80 in Eppendorf tubes. The tubes were placed vertically without shaking and incubated at 37 °C for 4 weeks. At a pre-determined time intervals (1, 3, 6, 12, 24 and 72 h followed by 1, 2, 3 and 4 weeks), the samples were centrifuged at 3000 rpm for 3 min and the supernatant was withdrawn and replenished with an equal volume of fresh medium. The supernatant consisted of alpha-mangostin was diluted with 70% v/v acetonitrile, filtered through 0.2 μm PTFE microfilter and immediately analysed by a modified RP-HPLC as described by Pothitirat and Gritsanapan (2009). Data were expressed as the mean percentage of cumulative release ± standard deviation ($n = 3$).

Differential scanning calorimetry

The physical nature of alpha-mangostin and glass transition temperature (T_g) of the PLGA before and after the microencapsulation process were determined using differential scanning calorimetry (DSC 1, STARe System, Mettler Toledo, Greifensee, Switzerland). Briefly, 5 mg of each sample were accurately weighed into a 40 μl, pin-holed aluminium crucibles and hermetically sealed. All measurements were operated against a reference of similar geometric and size of an empty pin-holed, hermetically sealed aluminium crucible. The crucibles were isothermally equilibrated for 5 min at 0 °C to ensure isothermal starting conditions. Then, a re-conditioning process was performed by gradual heating from 0 to 85 °C followed by quench-cooling to −20 °C in order to remove any sample history (Rouse et al., 2007). Then, the crucibles were heated again to 250 °C. All heating were conducted at the same rate, i.e. 10 °C/min. The scanning was conducted under nitrogen purge at flow rate of 1 ml/min. The thermograms were analysed using Mettler STAR^e software (version 9.10) (Mettler Toledo, Greifensee, Switzerland), and the T_g was expressed as onset, midpoint and endpoint temperatures.

FTIR spectroscopy

FTIR spectroscopy was performed to assess the interaction between alpha-mangostin and PLGA copolymer using Fourier transform infrared spectrometer (Spectrum 100, Perkin-Elmer Ltd, England, UK). The spectra of samples were analyzed over a range of 400–4000 cm^{-1} at a resolution of 2 cm^{-1}. Total of 12

Journal of Microencapsulation Downloaded from informahealthcare.com by University of Laval on 05/25/14
For personal use only.

scans were performed for each sample using built-in standard software package.

Results and discussion

Analysis of model

Multiple emulsion solvent evaporation technique for microencapsulation of lipophilic therapeutic agents into PLGA is rarely being reported as the protocol of choice perhaps due to low affinity between relatively hydrophilic PLGA and the agent. In this study, we had proved that it was feasible to encapsulate lipophilic agent employing PVA as stabilizer with desirable size distribution intended for pulmonary delivery. Since stability of primary emulsion during the preparation of double emulsion process is crucial to ensure substantially high EE (Mohamed and Van Der Walle, 2008), different independent variables that may influence its stability had been identified and manipulated to investigate their effects on the responses using RSM. As shown in Table 2, 30 runs tailored in Face CCD was accomplished and the mathematical relationships were generated between the independent variables addressed as second-order polynomial equation using multi-linear regression analysis in order to envisage the relevant responses. The following were the generated models:

$$\begin{aligned} Y1 = {} & 30.49 - 1.09X_1 + 1.70X_2 - 0.52X_3 - 0.43X_4 \\ & - 0.42X_1X_2 - 1.10X_1X_3 - 0.99X_1X_4 \\ & - 0.065X_2X_3 - 0.16X_2X_4 - 0.077X_3X_4 \\ & + 1.52X_1^2 + 2.20X_2^2 - 4.26X_3^2 \end{aligned} \quad (4)$$

$$\begin{aligned} Y2 = {} & 2.02 + 0.096X_1 - 0.005X_2 + 0.056X_3 - 0.020X_4 \\ & - 0.056X_1X_2 - 0.071X_1X_3 + 0.049X_1X_4 \\ & + 0.021X_2X_3 - 0.047X_2X_4 + 0.001X_3X_4 \\ & - 0.19X_1^2 + 0.11X_2^2 - 0.29X_3^2 \end{aligned} \quad (5)$$

$$\begin{aligned} Y3 = {} & 0.97 + 0.031X_1 - 0.007X_2 + 0.097X_3 - 0.034X_4 \\ & - 0.080X_1X_2 + 0.013X_1X_3 + 0.058X_1X_4 \\ & + 0.078X_2X_3 + 0.006X_2X_4 + 0.069X_3X_4 \\ & - 0.099X_1^2 - 0.017X_2^2 - 0.085X_3^2 \end{aligned} \quad (6)$$

where *Y*1, *Y*2 and *Y*3 refer to EE, PS and polydispersibility index (SPAN), respectively, as the responses. The factors including PVA concentration, ratio of oil to aqueous phase and sonication time for both primary and secondary emulsion were represented in the equations as X_1, X_2, X_3 and X_4, respectively.

Following the 30 runs, the data were analyzed by analysis of variance (ANOVA) with multiple regression analysis and three-dimensional response surface plots were generated based on the reduced polynomial equations, which contain only the statistically significant terms to visualize the significant manipulating impact of the variables on the responses (Gohel and Amin, 1998). It was found that PVA concentration (X_1) and the ratio of oil to water phase (X_2) in primary emulsion exhibited extremely significant ($p < 0.001$) effects on the EE. However, interaction between those two did not appear to significantly affect the EE. In contrast, sonication time of both primary and secondary emulsion seems to insignificantly affect EE individually. However, interaction between PVA concentration and sonication time of primary emulsion seems to significantly ($p < 0.05$) influence EE as

Table 2. Face CCD lay out with the responses values.

	Independent variables				Responses ± SD		
Run	X_1	X_2	X_3	X_4	EE (%)	PS (μm)	SPAN
1	−1	−1	−1	−1	27.08 ± 0.015	1.68 ± 0.043	0.90 ± 0.047
2	−1	−1	−1	1	30.37 ± 0.016	1.57 ± 0.023	0.26 ± 0.033
3	−1	−1	1	−1	30.23 ± 0.040	1.91 ± 0.006	0.72 ± 0.019
4	−1	−1	1	1	26.85 ± 0.024	1.89 ± 0.006	0.70 ± 0.004
5	−1	0	0	−1	32.34 ± 0.020	1.82 ± 0.017	0.94 ± 0.008
6	−1	0	0	1	32.55 ± 0.005	1.63 ± 0.133	0.91 ± 0.104
7	−1	1	−1	−1	33.53 ± 0.033	1.85 ± 0.006	0.91 ± 0.004
8	−1	1	−1	1	32.21 ± 0.023	1.70 ± 0.006	0.41 ± 0.003
9	−1	1	1	−1	33.58 ± 0.035	2.06 ± 0.017	0.95 ± 0.009
10	−1	1	1	1	35.30 ± 0.016	1.87 ± 0.059	0.91 ± 0.041
11	0	−1	0	−1	30.61 ± 0.009	2.07 ± 0.072	1.02 ± 0.039
12	0	−1	0	1	36.14 ± 0.015	2.19 ± 0.031	0.96 ± 0.026
13	0	0	−1	−1	25.20 ± 0.037	1.80 ± 0.010	0.85 ± 0.006
14	0	0	−1	1	27.44 ± 0.113	2.01 ± 0.006	0.92 ± 0.008
15	0	0	0	−1	29.20 ± 0.063	2.18 ± 0.015	0.87 ± 0.003
16	0	0	0	1	25.96 ± 0.023	1.82 ± 0.075	0.91 ± 0.021
17	0	0	1	−1	27.64 ± 0.044	2.20 ± 0.006	0.89 ± 0.002
18	0	0	1	1	26.73 ± 0.117	1.99 ± 0.159	0.99 ± 0.089
19	0	1	0	−1	32.08 ± 0.061	2.14 ± 0.010	0.93 ± 0.009
20	0	1	0	1	34.66 ± 0.039	2.16 ± 0.173	1.01 ± 0.103
21	1	−1	−1	−1	28.63 ± 0.036	2.09 ± 0.006	0.91 ± 0.003
22	1	−1	−1	1	27.39 ± 0.042	2.23 ± 0.006	0.89 ± 0.005
23	1	−1	1	−1	26.43 ± 0.015	1.85 ± 0.006	0.91 ± 0.008
24	1	−1	1	1	24.26 ± 0.028	2.10 ± 0.021	0.92 ± 0.005
25	1	0	0	−1	38.03 ± 0.027	1.84 ± 0.001	0.86 ± 0.001
26	1	0	0	1	27.20 ± 0.085	2.06 ± 0.015	0.89 ± 0.003
27	1	1	−1	−1	35.32 ± 0.101	2.05 ± 0.044	0.57 ± 0.044
28	1	1	−1	1	29.68 ± 0.040	1.76 ± 0.006	0.40 ± 0.005
29	1	1	1	−1	27.50 ± 0.015	1.98 ± 0.128	0.93 ± 0.085
30	1	1	1	1	28.04 ± 0.013	1.99 ± 0.006	1.01 ± 0.023

Abbreviation: Standard deviation (SD), PVA concentration (X_1), ratio of oil to aqueous phase (X_2), sonication time for primary emulsion (X_3), sonication time for secondary emulsion (X_4), encapsulation efficiency (EE), particle size (PS), polydispersibility index (SPAN), low factorial level (−1), centre point level (0) and high factorial level (1).

Journal of Microencapsulation Downloaded from informahealthcare.com by University of Laval on 05/25/14
For personal use only.

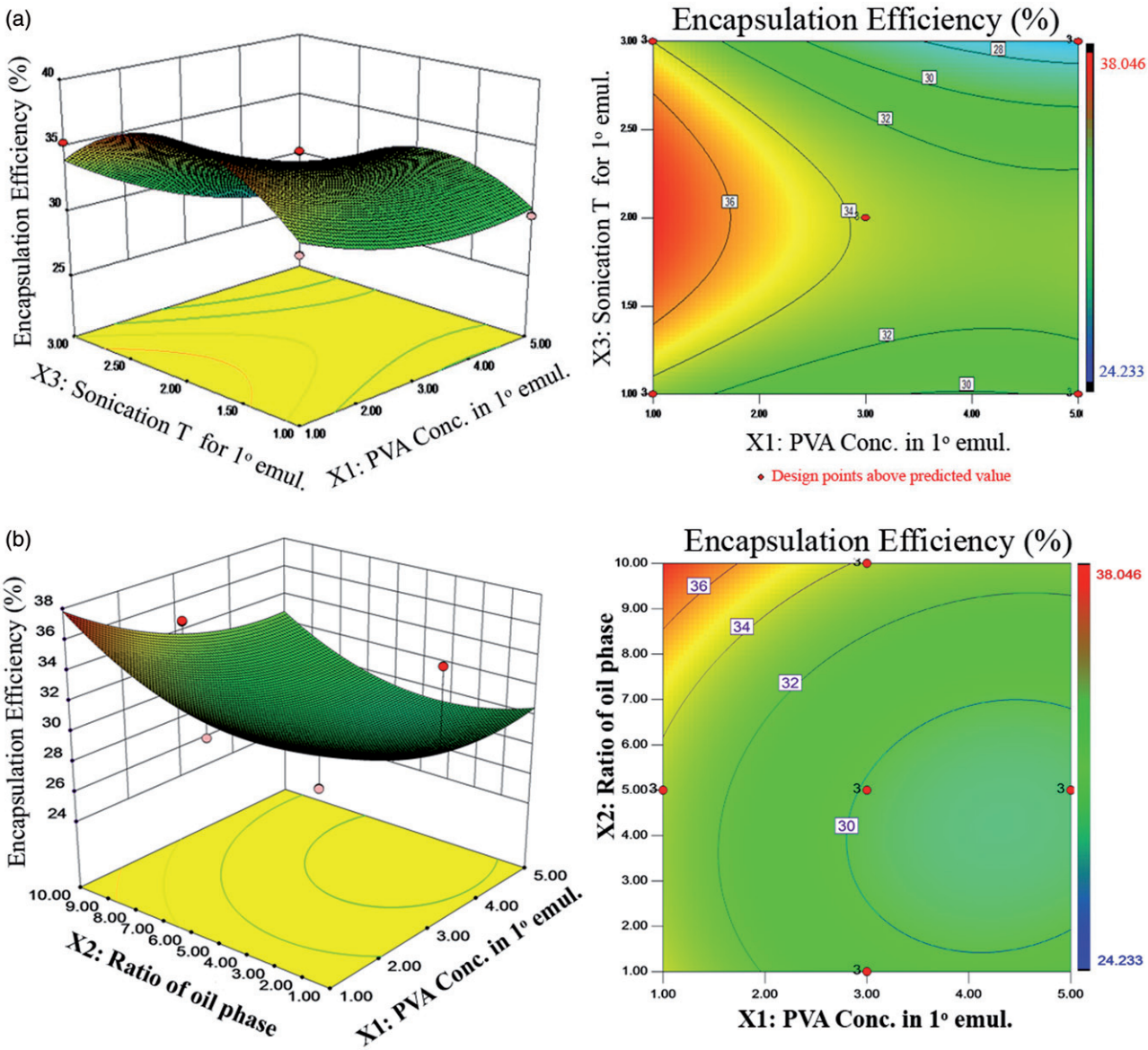

Figure 1. (a) Three-dimensional response surface plot (left) with its corresponding contour plot (right) of the alpha-mangostin microspheres prepared at constant high level 1 for both sonication time of secondary emulsion (5 min) and ratio of oil phase (10:1). The encapsulation efficiency was at highest (more than 36%) at red region of the plot (middle left corner) corresponds to lowest level of PVA concentration (less than 2%) with intermediate to highest level of sonication time for primary emulsion (1.5–3 min). (b) Three-dimensional response surface plot (left) with its corresponding contour plot (right) of the loaded microspheres prepared at constant centre point 0 level for primary emulsion sonication time (2 min) but at high level 1 for secondary emulsion sonication time (5 min). The encapsulation efficiency was at highest (more than 36%) at red region of the plot (uppermost left corner) corresponds to highest ratio of oil phase 1:10 but at lowest concentration of PVA (1% w/v).

depicted in RSM plots (Figure 1a). The RSM plots (Figure 1a and b) also suggest that PVA concentration and ratio of oil phase are the most critical factor to consider to achieve highest EE. Having said that, the highest achievable here by using PVA as stabiliser and surfactant was approximately 36–38%, which is relatively poor EE compared to other PLGA microspheres with different encapsulated agent (Mohamed and van der Walle, 2006). This may be attributed to low affinity of alpha-mangostin and xanthone for the polymer accelerating diffusion out from the oil phase to the external aqueous medium and precipitated in the form of crystals from the nascent microspheres (Barichello et al., 1999; Teixeira et al., 2005).

Surprisingly, the PS distributions or geometric diameter (1.48–2.26 μm) of all experimental runs were within desirable target range (<3 μm) suitable for deep inhalation. As attested by ANOVA, the PVA concentration and sonication time of primary emulsion showed extremely significant effect ($p < 0.001$) on the PS individually. In addition, interaction between the two factors significantly influences PS suggesting their critical role in determining optimum size for microspheres. Again, sonication time of secondary emulsion did not appear to significantly influence the PS. Based on the polynomial equation of the PS (Y2; Equation 5), it showed that PVA concentration had synergistic influence on the PS, i.e. the size increased with PVA concentration. It had been suggested that high concentration of PVA increased viscosity of the primary emulsion resulting in larger droplet size (Bouissou et al., 2006). In addition, desirable PS seems to be the easiest to achieve by the protocol employed maybe due temperature of sonication that was lowered since the sonication was conducted over the ice bath. Low temperature employed could minimise pre-mature hardening of microspheres that possibly attributed to increase rate of solvent evaporation facilitated at high temperature (Scholes et al., 1993).

Journal of Microencapsulation Downloaded from informahealthcare.com by University of Laval on 05/25/14
For personal use only.

Journal of Microencapsulation Downloaded from informahealthcare.com by University of Laval on 05/25/14
For personal use only.

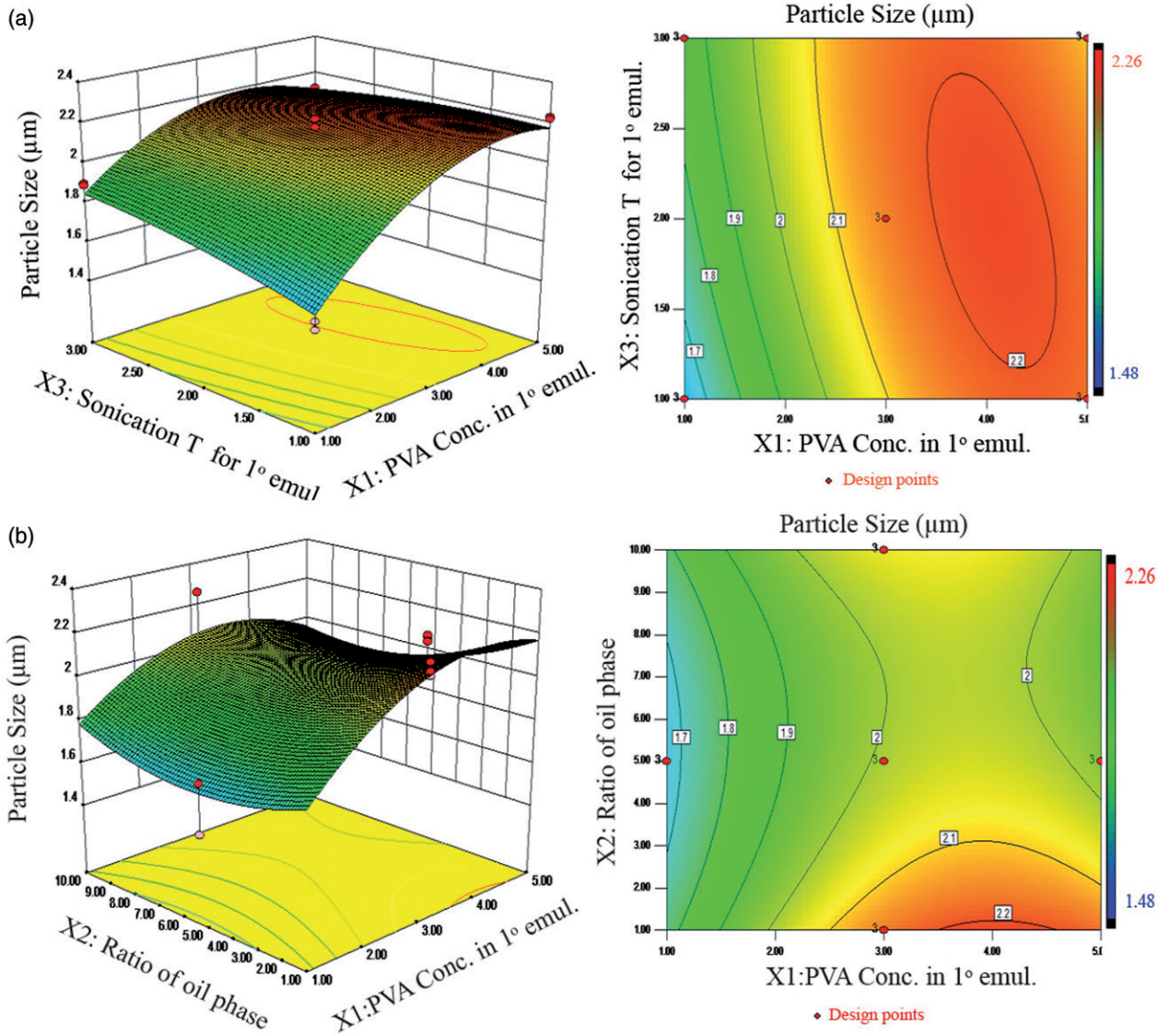

Figure 2. (a) Three-dimensional response surface plot (left) with its corresponding contour plot (right) of the loaded microspheres prepared at constant high level 1 for both sonication time of secondary emulsion (5 min) and ratio of oil phase (10:1). The particle size is within desirable geometric diameter (more than 2 µm) at red region of the plot (from middle to right side) corresponding to PVA concentration of 3–5% w/v and occurs throughout all levels of sonication time for primary emulsion. (b) Three-dimensional response surface plot (left) with its corresponding contour plot (right) of the loaded microspheres prepared at constant centre point 0 level for primary emulsion sonication time (2 min) but at high level 1 for secondary emulsion sonication time (5 min). The particle size was within desirable geometric diameter at red region of the plot (lower right corner) corresponding to lowest ratio of oil phase (1:1) but at PVA concentration of 3–5% w/v.

Looking at the 30 runs data, and RSM plots (Figure 2a and b), we concluded that desirable geometric PS could be obtained at all sonication time of primary emulsion and at relatively wide range of PVA concentration. Therefore, it seems that the factors tested in this study had less profound effect on the PS as compared to effect on the EE of alpha-mangostin microsphere.

Therefore, for optimize formulation, we had selected the following levels for PVA concentration, ratio of oil phase, sonication time of primary and secondary to be at −1, 1, 0 and 1, respectively. The RSM plots (Figure 2a and b) reveals that PVA-desirable geometric PS could be despite having insignificant influence on EE and PS, sonication time of secondary emulsion seems to play an important role in producing almost monodisperse (desirable span value of less than 0.5) microspheres. As reflected by Equation (6), this sonication time has antagonistic effects on span value in such a way that the high level (5 min) produced small span value as corroborated by the RSM plots (Figure 3a and b). Based on ANOVA, PVA concentration had less significant effect compared to both sonication time of primary and secondary emulsion. Comparing span values of all 30 runs, we concluded that the optimum level for sonication time of primary and secondary emulsion were 2 and 5 min, respectively, for desirable span values of less than 0.5.

Overall, the results suggested that optimized formulation of alpha-mangostin microspheres required the following factors, i.e. 1% w/v PVA concentration, 1:10 ratio of oil to aqueous phase in primary emulsion, 2 min sonication time for primary emulsion and 5 min for secondary emulsion (i.e. 1, 1, 0 and 1 levels).

Model validation

To check adequacy of the generated mathematical models for all responses, we had done check point analysis to validate the equations. The analysis plays a critical role to identify prediction strength of the polynomial equations that were obtained from multi linear regression analysis. The points were randomly selected within the high and low levels of the independent variables. Bias less than 10% reflect a validated and reliable

Journal of Microencapsulation Downloaded from informahealthcare.com by University of Laval on 05/25/14
For personal use only.

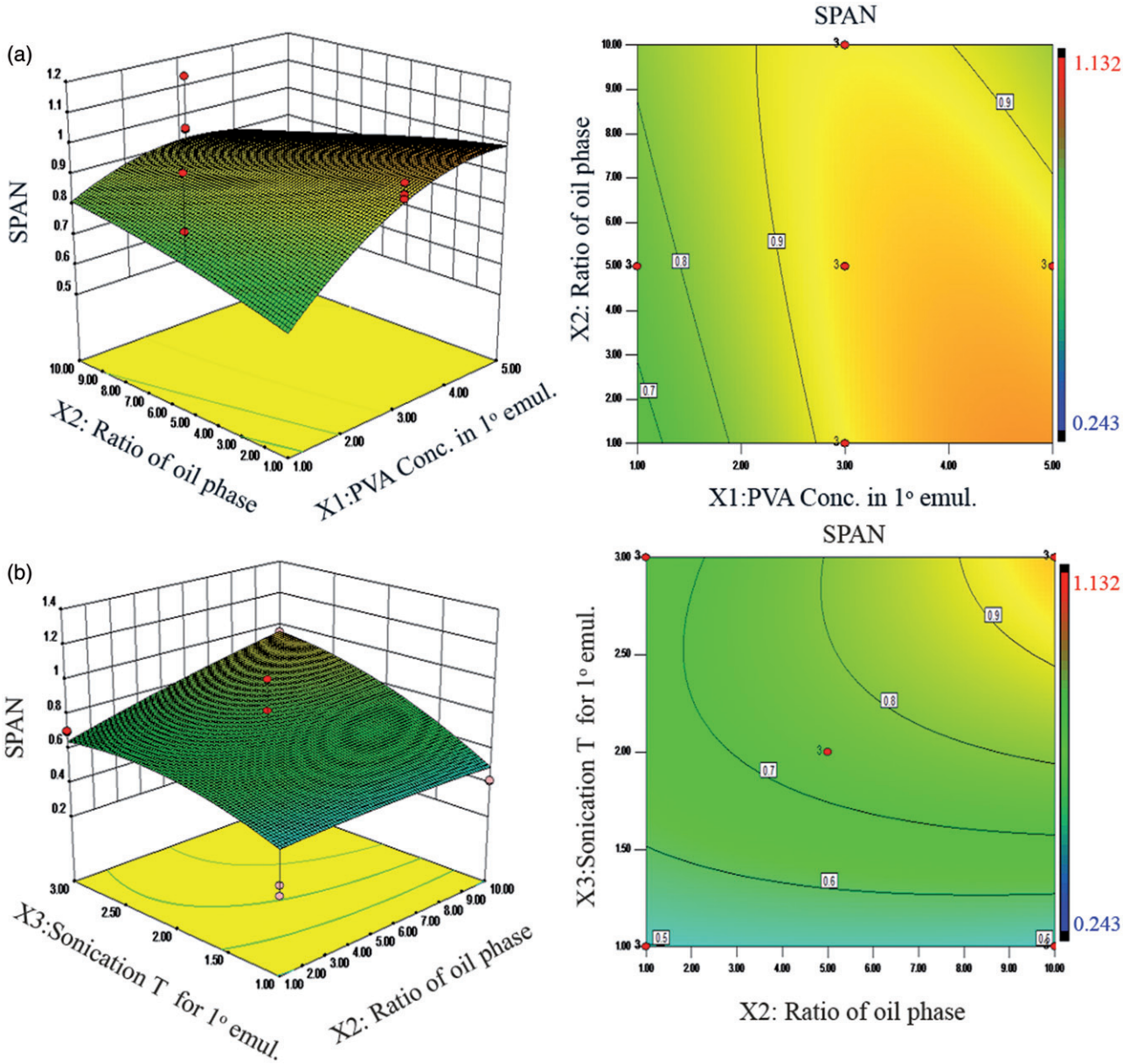

Figure 3. (a) Three-dimensional response surface plot (left) with its corresponding contour plot (right) of alpha-mangostin microspheres prepared at constant centre point, high level of sonication time primary emulsion (2 min) and at high level 1 for secondary emulsion (5 min). The microspheres prepared were almost monodisperse (span less than 0.5) at green to blue region of the plot (one-third of left plot), which occur for all ratio of oil phase at PVA concentration less than 2% w/v. (b) Three-dimensional response surface plot (left) with its corresponding contour plot (right) of alpha-mangostin microspheres prepared at constant high level 1 for sonication time of secondary emulsion (5 min) and at low level of PVA concentration (1% w/v). The microspheres obtained were almost monodisperse at green to blue region of the plot (all area), suggesting that monodispersity could probably be achieved at all ratio of oil and at all level of sonication time of primary emulsion.

Table 3. Model adequacy validation using check points analysis for encapsulation efficiency (Y_1).

	Factors						
Run	X_1	X_2	X_3	X_4	Predicted value (Y_1)	Experimental value (Y_1) ± SD	Bias (%)
1	−1	−1	0	−1	32.45	32.78 ± 0.014	1.01
2	−1	1	0	1	37.82	39.12 ± 0.006	3.32
3	0	−1	−1	1	26.99	29.82 ± 0.086	9.49
4	0	1	−1	−1	31.22	30.73 ± 0.017	1.59
5	1	−1	0	1	30.58	29.88 ± 0.43	2.34

predictive model (Ricci et al., 2006; Nasr et al., 2011). With respect to EE (Y_1), a good agreement between the experimental and predicted values was observed as shown in Table 3. It is clear that the calculated biases for all experiments were less than 10%, which implies that the EE model (Equation 4) was valid and reliable. Similarly, the experimental values for PS were extremely close to the corresponding predicted values (bias <10%; Table 4). Hence, both mathematical models for EE (Equation 4) and PS (Equation 5) could be employed for optimization of microencapsulation of alpha-mangostin.

In contrast, the biases for SPAN were found to be inconsistent, with some extreme values laid outside 10% limit. This implies that the mathematical model for this factor is less predictable and less reliable to be used for optimization process, hence exclusion of this factor.

Optimization

In order to obtain a formula with maximum EE, minimum PS and narrow SPAN, the levels of the independent variables were optimized by graphical and numerical analysis using Design-Expert® software based on the criterion of desirability (Zu et al., 2009). The desirability is defined as an objective function having scores range from zero to one. Zero indicates that the predicted response is outside the limit, whereas value one reflects targeted response value (Ibrahim et al., 2010). As such, for EE that had a desirability score of 0.98, the predicted response was differing from experimental value by only 0.02% (Table 5). Similarly, since the PS had a desirability score of 0.61, the predicted response for the PS was less than 0.5% confirming good agreement between mathematical models and experimental value.

The optimized microspheres formula loaded with α-mangostin was prepared with 1% (w/v) PVA, 10:1 (v/v) volume ratio of oil to aqueous phase, 2 and 5 min sonication for primary and secondary emulsion, respectively. The total desirability of this formulation was 0.77, which refer to weighted geometric average of all responses desirability as stated by Ibrahim et al. (2010) and hence indicates mathematical models generated from 30 runs here are valid and predictive tools for optimization.

External morphology and theoretical aerodynamic diameter

As shown in Figure 4(A), protocol employed yielded spherical, non-aggregated, non-porous smooth surfaces alpha-mangostin microspheres. The results is coherent with overall span values (less than 0.5) obtained in the 30 runs suggesting almost monodisperse particles produced regardless of levels of the independent variables. The microspheres, however, is unstable against higher voltage of electron beam (magnification 17 000×) disrupting its surfaces (Figure 4B) at higher magnification Figure 4(B).

Following tapping of 5000×, the volume occupied per 175 mg of lyophilized alpha-mangostin microspheres (2.06 ± 0.017 µm) were found to be 1.2 ml. Therefore, the aerodynamic diameter (d_a) was 784.3 ± 7.5 nm, which is desirable range for fine particle fraction (FPF; aerodynamic diameter less than 5 µm, as recommended by Britich Pharmacopoeia). This FPF value had also been employed by other researchers that consider 30–40% FPF as efficient aerosolised particles (Fiegel et al., 2004; Zeng et al., 2007). The value in this study is a useful indicator prior to determination of FPF using suitable cascade impactor like Next

Table 4. Model adequacy validation using check points analysis for particle size (Y_2) and polydispersity index (Y_3).

	Factors				Predicted responses		Experimental responses ± SD		Bias (%)	
Run	X_1	X_2	X_3	X_4	Y_2	Y_3	Y_2	Y_3	Y_2	Y_3
1	−1	−1	0	−1	1.81	0.85	1.72 ± 0.005	0.91 ± 0.003	5.23	6.59
2	−1	0	1	1	1.76	0.80	1.71 ± 0.006	0.88 ± 0.003	2.92	9.09
3	−1	1	0	−1	2.02	0.99	1.87 ± 0.006	0.86 ± 0.003	8.02	15.12
4	0	−1	1	−1	2.11	0.87	2.10 ± 0.153	1.05 ± 0.131	0.48	17.14
5	0	1	−1	−1	2.10	0.79	2.04 ± 0.173	0.99 ± 0.086	2.94	20.20

Table 5. Predicted and observed responses for the optimized formulation with their individual desirability.

Response	Predicted value	Observed value ± SD	Bias (%)	Individual desirability
Encapsulation efficiency (%)	37.81	39.12 ± 0.01	3.44	0.98
Particle size (µm)	1.78	2.06 ± 0.017	15.73	0.61
Polydispersibility index	0.81	0.95 ± 0.009	17.28	0.36

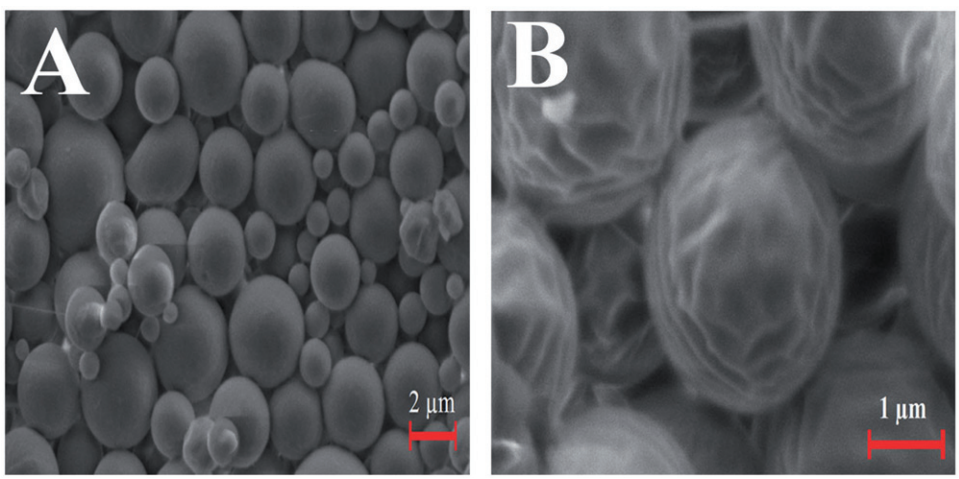

Figure 4. Microimages of optimized alpha-mangostin microspheres at different resolution: (A) 5000× mag; (B) 17 000 mag.

Journal of Microencapsulation Downloaded from informahealthcare.com by University of Laval on 05/25/14
For personal use only.

Journal of Microencapsulation Downloaded from informahealthcare.com by University of Laval on 05/25/14
For personal use only.

Generation Cascade Impactor. In addition, several strategies have been reported with regard to controlling and modulating surface morphology of microspheres, fabricated by solvent-evaporation and intended for pulmonary delivery. Huo et al. (2005) reported relatively large microspheres (5–30 μm) of smooth surface for pulmonary delivery which were stable for 3 months and although corresponding tapped density was not performed, these spheres would appear to be too large for effective deposition to the peripheral lung.

In vitro release study

As mentioned earlier, although the loaded alpha-mangostin into PVP nanomicelles revealed highest aqueous solubility (~2.7 mg/ml) as compared to its counterpart free alpha-mangostin (~200 ng/ml), the *in vitro* release profile of alpha-mangostin from these nanocarriers was not addressed due to strong hydrogen bonding between the polymer and alpha-mangostin (Aisha et al., 2012). Therefore, in this study we used Tween 80 solution to confer the ''sink condition'' during the release essay as employed by other independent study (Ji et al., 2012). 0.1% Tween 80 and other surfactant have been employed in many other studies to cause sink condition based on its ability to reduce the interfacial tension of the freeze-dried particles and cause full hydration of the particles. The concentration of surfactant used was based on critical micelle concentration of Tween 80 and other sorbitan-based group which is very low, approximately 0.005% v/v. Presence of the surfactant also improves aqueous solubility of the alpha-mangostin, which indirectly evidenced by the absorbance data. One millilitre volume was used to ensure quantifiable amount of extracted alpha-mangostin from the PLGA microspheres up to 1 month release.

As these microspheres were intended for pulmonary delivery, it is expected that these particle will be deposited in the lung region (esp. alveolar and some maybe deposited in tracheobronchial region) and started releasing the alpha-mangostin there upon contact with lung surfactant or other enzymes and mucous. These lung regions are not having as high magnitude of muscular movement as those in gastrointestinal tract neither the lung environment have that active secretion of bile acid/gastro fluid. Hence, the best release simulation is a stagnant condition rather than shaken. The condition is also to ensure the release is absolutely due to the ability of PLGA to degrade upon contact with water and simultaneously release the therapeutic agents, and not due to other external factors facilitating the degradation.

The *in vitro* release profile of alpha-mangostin from the optimized alpha-mangostin microspheres exhibited a typical triphasic pattern attributed to PLGA degradation profile as shown in Figure 5. The mathematical analysis of the release curve revealed logarithmic model. The first stage commenced with an initial burst release of ~33.9 μg/ml corresponding to 7.7% of the total entrapped alpha-mangostin in the first 1 h. The burst release effect had been reported in numerous PLGA microsphere preparations regardless of agents being encapsulated, be it macromolecules (Mohamed and van der Walle, 2006; Mao et al., 2007) and small molecules (Liu et al., 2004; Xu and Czernuszka, 2008). It appears that this natural product-based alpha-mangostin also exhibited similar release profile, and this may implied that hydro or lypophilicity of the encapsulating agents may not play role in causing the burst effects. It was suggested that the burst effect was predominantly due to precipitating encapsulated agents on the surface of microspheres, which were formed during thermodynamically transient phases of nascent microspheres (Xu and Czermuska, 2008). The second release phase lasted for about 72 h, which was likely to follow first-order kinetic release with a total cumulative amount of 26.1%. Subsequent to this release was the third release phase that lasted for 28 days. At the end of the experiment, about 44.4% of alpha-mangostin was released from PLGA microspheres. It is noteworthy that the release measured over the entire 4 weeks did not result in complete release of alpha-mangostin, which implied that total degradation time of this PLGA (IV 0.4 dl/g) may take longer than 4 weeks to completely degrade releasing all entrapped alpha-mangostin. Besides, the sustained-release of alpha-mangostin may also be due to polymer entanglement and some interaction between alpha-mangostin and the PLGA, as evident by the FTIR spectra (Figure 7).

In vitro cytotoxicity

Human non-small lung adenocarcinoma cells (A549) line had been documented to exert characteristic type II pulmonary

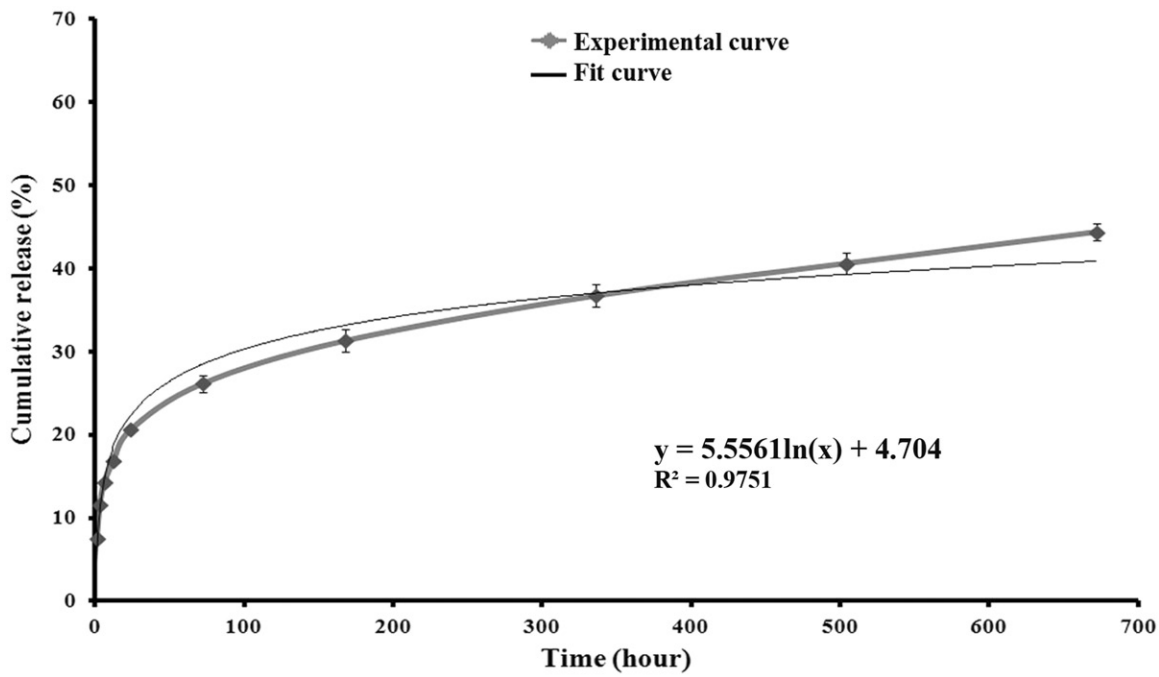

Figure 5. The *in vitro* release profile of the optimized formulation of alpha-mangostin-PLGA microspheres; $n = 3$.

Table 6. Glass transition temperature(T_g), *in vitro* release and cytotoxicity results.

	T_g (°C)			*In vitro* release (%)		
Sample	Onset	Midpoint	Endpoint	Burst effect	Release after 48 h.	IC_{50} (μM)
Alpha-mangostin (AM)	n/a	n/a	n/a	–	–	12.88 ± 2.437
AM-PLGA microspheres	43.96	45.33	47.303	7.48 ± 0.309	26.21 ± 0.663	17.73 ± 2.865
Blank microspheres	43.34	45.06	46.87	–	–	–
PLGA (raw)	40.87	42.44	44.10	–	–	–

Results were analysed using paired *t*-test to compare significant difference between the IC_{50}. Free alpha-mangostin did not exhibit T_g phase but instead a melting point peak at 181.4 °C.

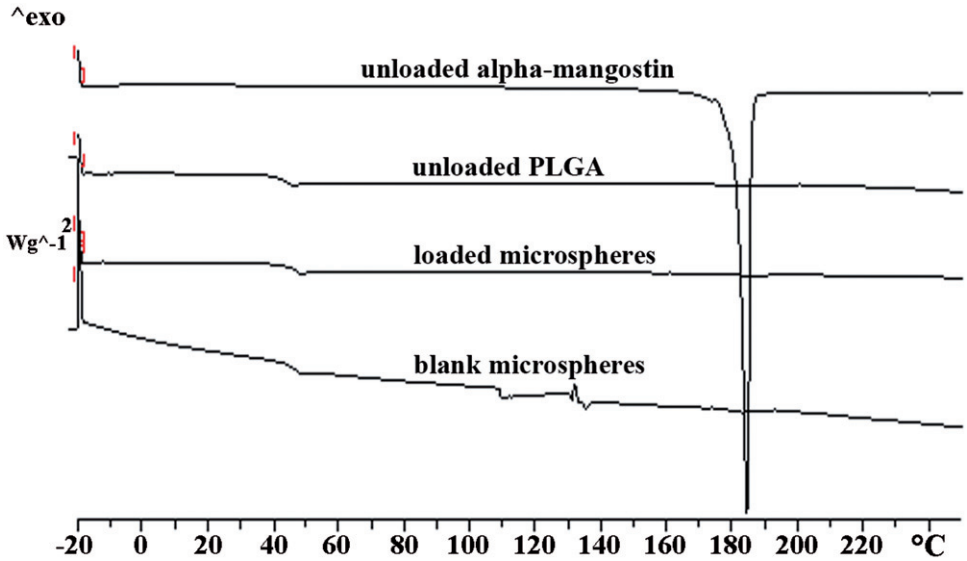

Figure 6. Thermograms of free alpha-mangostin, unloaded PLGA, loaded and blank microspheres.

epithelial cells, and it may play a substantial role as drug barriers to pulmonary delivery (Foster et al., 1998). As such, the cytotoxicity of alpha-mangostin before and after it was entrapped into PLGA microspheres were determined against this cell line using MTT assay. We found that our free alpha-mangostin exhibited IC_{50} of 12.88 μM (Figure 7), which was in good agreement to the previously reported value (Shih et al., 2010). However, the inhibition of cell growth by free alpha-mangostin was significantly higher ($p < 0.05$) than alpha-mangostin loaded-PLGA microspheres (Table 6). The result indicated that microencapsulation had significantly reduced its efficacy to inhibit cell growth.

Differential scanning calorimetry

The thermal behaviour for both free alpha-mangostin and PLGA copolymer was investigated before and after the microencapsulation process in order to delineate any physical changes that may occur post-encapsulation. As shown in Figure 6, alpha-mangostin exhibited a sharp endothermic peak at 181.4 °C, which was attributed to its melting point. However, this peak disappeared from the thermogram of alpha-mangostin PLGA microspheres. Similar result was previously reported by Aisha et al. (2012) when they dispersed the alpha-mangostin in a water-soluble polymer. These data suggest that encapsulation of alpha-mangostin into PLGA microspheres had changed its physical nature from crystalline to amorphous state, which in turn leads to enhance its aqueous solubility (Teixeira et al., 2005). The latter is desirable since it is related to bioavailability of the alpha-mangostin, which is envisaged to be increased as well at the vicinity of any absorbing membrane, which include alveolar region.

Free PLGA copolymer with a molecular weight of 34 kDa (IV 0.4 dl/g) showed a T_g onset at 40.9 °C which was increased post-encapsulation based on the T_g exhibited by the alpha-mangostin PLGA microspheres and the blank microsphere (Table 6). The slight increase in temperature maybe suggestive of anti-plasticizing effect caused by residual PVA in the microspheres that was also previously reported by other independent study (Bouissou et al., 2006). Looking closer, the anti-plasticizing effect seemed to be higher in alpha-mangostin PLGA microsphere compared to blank microsphere, and this slight increase may also be contributed from the presence of hydrogen bonding between PLGA and the alpha-mangostin as evident by the FTIR spectra (Figure 8). However, the slight increase in T_g may also preclude any dominant influence as a result of experimental circumstances on the PLGA molecular structure.

FTIR spectroscopy

Functional groups analyses were assessed using FT-IR spectroscopy to determine possible molecular interaction between the alpha-mangostin and PLGA copolymer. Figure 8 shows the fingerprint spectrum of free alpha-mangostin produced broad peaks at 3408.2 cm^{-1} and 3251.5 cm^{-1}, which refer to the vibrational stretching of hydroxyl groups. In addition, the characteristic absorption bands for CH_3, C–O and prenyl groups were observed at 2910.1, 1050.1 and 1639.6 cm^{-1}, respectively. In contrast, these bands were disappeared when alpha-mangostin was entrapped into PLGA microspheres. These data were in good agreement with alpha-mangostin spectrum that was previously reported (Aisha et al., 2012). With respect to free PLGA, blank and alpha-mangostin loaded-PLGA microspheres spectra, the

Journal of Microencapsulation Downloaded from informahealthcare.com by University of Laval on 05/25/14
For personal use only.

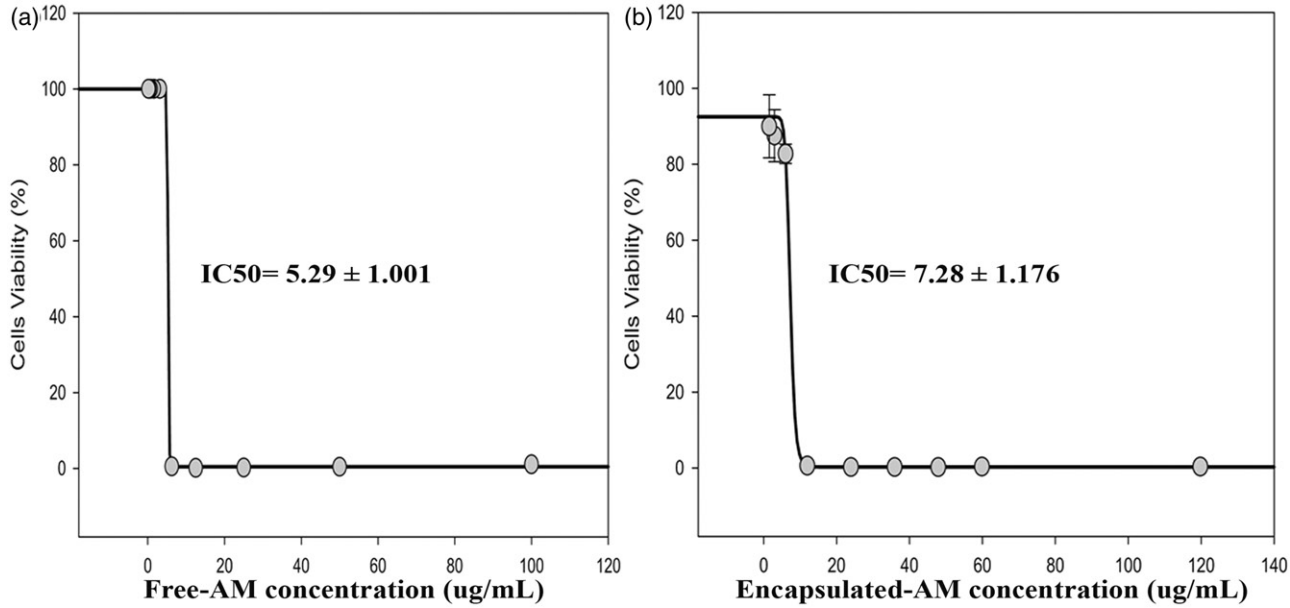

Figure 7. Plots showing IC_{50} of (a) free alpha-mangostin and (b) encapsulated alpha-mangostin. AM: alpha-mangostin.

Figure 8. FTIR spectra of the free forms of PLGA, alpha-mangostin and polyvinyl alcohol before microencapsulation process compared to the blank and loaded microspheres.

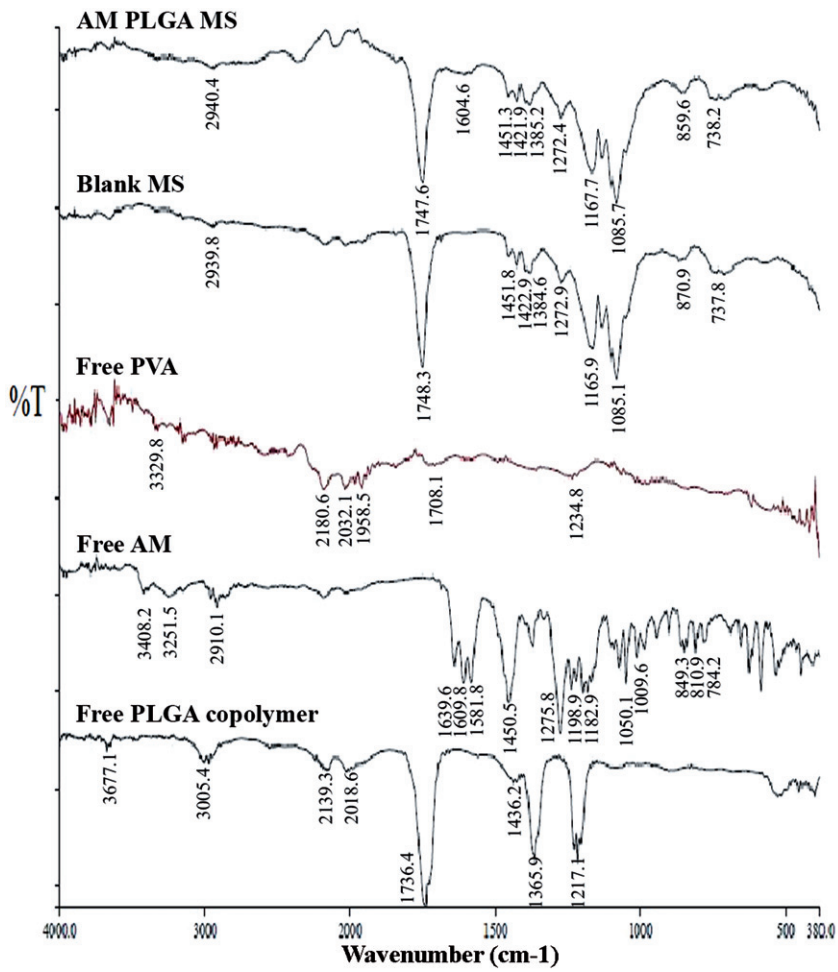

triple transmission peaks that were observed in the range of 1400–1500 cm^{-1} refer to glycolide and lactide of PLGA polymer, whereas the vibrational stretching of free PLGA carbonyl groups appeared at 1736.4 cm^{-1} which shifted to 1748.3 and 1747.6 cm^{-1} the spectra of blank and loaded microspheres, respectively (Liu et al., 2004; Xu and Czermuska, 2008). The FTIR spectra of both blank and loaded microspheres exhibited almost similar pattern; however, the only difference was detected at 1604.6 cm^{-1} suggestive of alpha-mangostin existence. These results indicate that microencapsulation had induced interaction between hydroxyl groups of alpha-mangostin to form hydrogen bonds with PLGA carbonyl groups. In addition, although PVA

Journal of Microencapsulation Downloaded from informahealthcare.com by University of Laval on 05/25/14
For personal use only.

was suggested to act as anti-plasticiser, however, the residual amount maybe minute enough to cause any molecular changes on the PLGA structure, as evident by the FTIR spectra.

Conclusion

Alpha-mangostin as a hydrophobic natural product-based compound was successfully encapsulated in PLGA microspheres using the solvent evaporation method, however, with relatively low EE. The experimental parameters were optimized by factorial CCD that produced formulation with desirable properties. The concentration of PVA in the internal aqueous phase and the volume of the oil phase for the primary emulsion play a critical role to control the EE. The PS of the microspheres and polydispersity were affected by the PVA concentration and emulsification time for primary emulsion. Longer emulsification time for secondary emulsion yielded microspheres with narrow SPAN. It was also found that microencapsulation had changed crystalline to amourphous alpha-mangostin that is expected to have better water solubility, at the expense of its efficacy to inhibit cell growth. However, since water solubility was thought to be enhanced, we expect that its bioavailability would be improved, which can only be proven by a pre-clinical study. The resultant PLGA microspheres may be used as a promising micro-carrier system to deliver alpha-mangostin to the lung cancer tissue.

Declaration of interest

The authors report no conflicts of interest. The authors alone are responsible for the content and writing of the article.

This work was funded by International Islamic University Malaysia (IIUM) (Grant ID: EDW B1002-350).

References

Aisha AFA, Ismail Z, Abu-Salah KM, Majid AMSA. Solid dispersions of α-mangostin improve its aqueous solubility through self-assembly of nanomicelles. J Pharm Sci, 2012;101(2):815–25.

Akao Y, Nakagawa Y, Nozawa Y. Anti-cancer effects of xanthones from pericarps of mangosteen. Int J Mol Sci, 2008;9:355–70.

Ali AAE, Taher M, Helaluddin ABM, Mohamed F. Development and validation of analytical method by RP-HPLC for quantification of alpha-mangostin encapsulated in PLGA microspheres. J Anal Bioanal Tech, 2012;3:7. doi: http://dx.doi.org/10.4172/2155-9872.1000155.

Barichello JM, Morishita M, Takayama K, Nagai T. Encapsulation of hydrophilic and lipophilic drugs in PLGA nanoparticles by the nanoprecipitation method. Drug Dev Indu Pharm, 1999;25:471–6.

Bouissou C, Potter U, Altroff H, Mardon H, Van Der Walle C. Controlled release of the fibronectin central cell binding domain from polymeric microspheres. J Control Release, 2004;95:557–66.

Bouissou C, Rouse J, Price R, Van der walle C. The influence of surfactant on PLGA microsphere glass transition and water sorption: Remodeling the surface morphology to attenuate the burst release. Pharm Res, 2006;23:1295–305.

Chen LG, Yang LL, Wang CC. Anti-inflammatory activity of mangostins from Garcinia mangostana. Food Chem Toxicol, 2008;46:688–93.

Cui J, Hu W, Cai Z, Liu Y, Li S, Tao W, Xiang H. New medicinal properties of mangostins: Analgesic activity and pharmacological characterization of active ingredients from the fruit hull of Garcinia mangostana L. Pharmacol Biochem Behav, 2010;95:166–72.

Emami J, Hamishehkar H, Najafabadi AR, Gilani K, Minaiyan M, Mahdavi H, Mirzadeh H, Fakhari A, Nokhodchi A. Particle size design of PLGA microspheres for potential pulmonary drug delivery using response surface methodology. J Microencapsul, 2009;26:1–8.

Fiegel J, Fu J, Hanes J. Poly (ether-anhydride) dry powder aerosols for sustained drug delivery in the lungs. J Control Release, 2004;96: 411–23.

Foster KA, Oster CG, Mayer MM, Avery ML, Audus KL. Characterization of the A549 cell line as a type II pulmonary epithelial cell model for drug metabolism. Exp Cell Res, 1998;243:359–66.

Gohel M, Amin A. Formulation optimization of controlled release diclofenac sodium microspheres using factorial design. J Control Release, 1998;51:115–22.

Huo D, Deng S, Li L, Ji J. Studies on the poly (lactic-co-glycolic) acid microspheres of cisplatin for lung-targeting. Int J Pharm, 2005;289: 63–7.

Ibrahim HM, Ahmed TA, Lila AEA, Samy AM, Kaseem AA, Nutan MTH. Mucoadhesive controlled release microcapsules of indomethacin: Optimization and stability study. J Microencapsul, 2010;27: 377–86.

Iikubo K, Ishikawa Y, Ando N, Umezawa K, Nishiyama S. The first direct synthesis of [alpha]-mangostin, a potent inhibitor of the acidic sphingomyelinase. Tetrahedron Lett, 2002;43:291–3.

Harun Ismail AF, Doolanea AM, Awang M, Mohamed F. High initial burst release of gentamicin formulated as PLGA microspheres implant for treating orthopaedic infection. Int J Pharm Pharm Sci, 2012;4(Suppl. 4):685–91.

Jemal A, Bray F, Center MM, Ferlay J, Ward E, Forman D. Global cancer statistics. CA Cancer J Clin, 2011;61(2):69–90.

Ji X, Gao Y, Chen L, Zhang Z, Deng Y, Li Y. Nanohybrid systems of non-ionic surfactant inserting liposomes loading paclitaxel for reversal of multidrug resistance. Int J Pharm, 2012;422:390–97.

Jung, HA, Su BN, Keller WJ, Mehta RG, Kinghorn AD. Antioxidant xanthones from the pericarp of *Garcinia mangostana* (Mangosteen). J Agric Food Chem, 2006;54:2077–82.

Kaomongkolgit R, Jamdee K, Chaisomboon N. Antifungal activity of alpha-mangostin against Candida albicans. J Oral Sci, 2009;51:401–6.

Liu DZ, Chen, WP, Lee CP, Wu SL, Wang YC, Chung TW. Effects of alginate coated on PLGA microspheres for delivery tetracycline hydrochloride to periodontal pockets. J Microencapsul, 2004;21:643–52.

Mahabusarakam W, Proudfoot J, Taylor W, Croft K. Inhibition of lipoprotein oxidation by prenylated xanthones derived from mangostin. Free Radic Res, 2000;33:643–59.

Mao S, Xu J, Cai C, Germershaus O, Schaper A, Kissel T. Effect of WOW process parameters on morphology and burst release of FITC-dextran loaded PLGA microspheres. Int J Pharm, 2007;334(1–2):137–48.

Mohamed F, van der Walle CF. PLGA microcapsules with novel dimpled surfaces for pulmonary delivery of DNA. Int J Pharm, 2006;311(1–2): 97–107.

Mohamed F, van der Walle CF. Engineering biodegradable polyester particles with specific drug targeting and drug release properties. J Pharm Sci, 2008;97:71–87.

Mosmann T. Rapid colorimetric assay for cellular growth and survival: Application to proliferation and cytotoxicity assays. J Immunol Methods, 1983;65:55–63.

Murphy TD. 2007. Response surface methodology for validation of oral dosage forms. In: Torbeck LD, ed. Pharmaceutical and medical device validation by experimental design. New York: Informa Healthcare.

Nasr M, Awad GAS, Mansour S, Al shamy A, Mortada ND. A reliable predictive factorial model for entrapment optimization of a sodium bisphosphonate into biodegradable microspheres. J Pharm Sci, 2011; 100:612–21.

Pedraza-Chaverri J, Reyes-Fermin LM, Nolasco-Amaya EG, Orozco-Ibarra M, Medina-Campos ON, Gonzalez-Cuahutencos O, Rivero-Cruz I, Mata R. ROS scavenging capacity and neuroprotective effect of alpha-mangostin against 3-nitropropionic acid in cerebellar granule neurons. Exp Toxicol Pathol, 2009;61:491–501.

Pothitirat W, Gritsanapan W. HPLC quantitative analysis method for the determination of α-mangostin in mangosteen fruit rind extract. Thai J Agri Sci, 2009;42:7–12.

Ricci M, Giovagnoli S, Blasi P, Schoubben A, Perioli L, Rossi C. Development of liposomal capreomycin sulfate formulations: Effects of formulation variables on peptide encapsulation. Int J Pharm, 2006; 311:172–81.

Rouse JJ, Mohamed F, van der Walle CF. Physical ageing and thermal analysis of PLGA microspheres encapsulating protein or DNA. Int J Pharm, 2007;339(1–2):112–20.

Sakagami Y, Iinuma M, Piyasena KG, Dharmaratne HR. Antibacterial activity of alpha-mangostin against vancomycin resistant Enterococci (VRE) and synergism with antibiotics. Phytomedicine, 2005;12:203–8.

Scholes P, Coombes A, Illum L, Daviz S, Vert M, Davies M. The preparation of sub-200 nm poly (lactide-co-glycolide) microspheres for site-specific drug delivery. J Control Release, 1993;25:145–53.

Shih YW, Chien ST, Chen PS, Lee JH, Wu SH, Yin LT. Alpha mangostin suppresses phorbol 12-myristate 13-acetate-induced MMP-2/MMP-9 expressions via avb3 integrin/FAK/ERK and NF-jB signaling pathway

Journal of Microencapsulation Downloaded from informahealthcare.com by University of Laval on 05/25/14
For personal use only.

in human lung adenocarcinoma A549 cells. Cell Biochem Biophys, 2010;58:31–44.

Suksamrarn S, Komutiban O, Ratananukul P, Chimnoi N, Lartpornmatulee N, Suksamrarn A. Cytotoxic prenylated xanthones from the young fruit of Garcinia mangostana. Chem Pharmaceut Bull, 2006;54:301–5.

Taher M, Susanti D, Rezali MF, Zohri FSA, Ichwan SJA, Alkhamaiseh SI, Ahmad F. Apoptosis, antimicrobial and antioxidant activities of phytochemicals from Garcinia malaccensis Hk.f. Asian Pac J Trop Med, 2012;5:136–41.

Tangpong J, Miriyala S, Noel T, Sinthupibulyakit C, Jungsuwadee P, St. Clair DK. Doxorubicin-induced central nervous system toxicity and protection by xanthone derivative of Garcinia Mangostana. Neuroscience, 2011;175:292–9.

Teixeira M, Alonso MJ, Pinto MMM, Barbosa CM. Development and characterization of PLGA nanospheres and nanocapsules containing xanthone and 3-methoxyxanthone. Eur J Pharm Biopharm, 2005;59: 491–500.

Wang Y, Xia Z, Xu JR, Wang YX, Hou LN, Qiu Y, Chen HZ. α-Mangostin, a polyphenolic xanthone derivative from mangosteen, attenuates β-amyloid oligomers-induced neurotoxicity by inhibiting amyloid aggregation. Neuropharmacology, 2012;62(2):871–81.

Williams P, Ongsakul M, Proudfoot J, Croft K, Beilin L. Mangostin inhibits the oxidative modification of human low density lipoprotein. Free Radic Res, 1995;23:175–84.

Wischke C, Schwendeman SP. Principles of encapsulating hydrophobic drugs in PLA/PLGA microparticles. Int J Pharm, 2008;364:298–327.

Wong HL, Bendayan R, Rauth AM, Li Y, Wu XY. Chemotherapy with anticancer drugs encapsulated in solid lipid nanoparticles. Adv Drug Deliv Rev, 2007;59:491–504.

Xu Q, Czernuszka JT. Controlled release of amoxicillin from hydroxyapatite-coated poly (lactic-co-glycolic acid) microspheres. J Control Release, 2008;127:146–53.

Yoo HS, Lee KH, Oh JE, Park TG. In vitro and in vivo anti-tumor activities of nanoparticles based on doxorubicin-PLGA conjugates. J Control Rel, 2000;68:419–31.

Zeng XM, MacRitchie HB, Marriott C, Martin GP. Huimidity-induced changes of the aerodynamic properties of dry powder aerosol formulations containing different carriers. Int J Pharm, 2007;333(1–2):45–55.

Zu Y, Zhang Y, Zhao X, Zhang Q, Liu Y, Jiang R. Optimization of the preparation process of vinblastine sulfate (VBLS)-loaded folate-conjugated bovine serum albumin (BSA) nanoparticles for tumor-targeted drug delivery using response surface methodology (RSM). Int J Nanomedicine, 2009;4:321–33.

Journal of Microencapsulation Downloaded from informahealthcare.com by University of Laval on 05/25/14
For personal use only.